

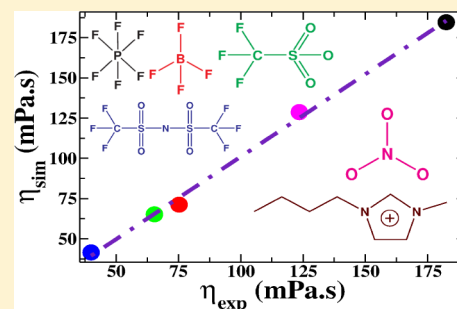
A Molecular Dynamics Study of Collective Transport Properties of Imidazolium-Based Room-Temperature Ionic Liquids

Anirban Mondal and Sundaram Balasubramanian*

Chemistry and Physics of Materials Unit Jawaharlal Nehru Centre for Advanced Scientific Research, Bangalore 560 064, India

Supporting Information

ABSTRACT: Transport properties of five room-temperature ionic liquids based on the 1-butyl-3-methylimidazolium cation with any of the following anions, $[\text{PF}_6]^-$, $[\text{BF}_4]^-$, $[\text{CF}_3\text{SO}_3]^-$, $[\text{NTf}_2]^-$, and $[\text{NO}_3]^-$, were determined from classical molecular dynamics simulations. The force field employed fractional ion charges whose magnitude were determined using condensed phase quantum calculations. Integrals of appropriate equilibrium time correlation functions within the Green–Kubo approach were employed to predict shear viscosity and electrical conductivity of these liquids. Computed shear viscosity values reproduce experimental data with remarkable accuracy. Electrical conductivity calculated for $[\text{BMIM}][\text{PF}_6]$ and $[\text{BMIM}][\text{BF}_4]$ showed impressive agreement with experiment while for $[\text{BMIM}][\text{CF}_3\text{SO}_3]$ and $[\text{BMIM}][\text{NTf}_2]$ the agreement is fair. The current approach shows considerable promise in the prediction of collective transport quantities of room temperature ionic liquids from molecular simulations.



INTRODUCTION

Room-temperature ionic liquids (RTILs) have shown considerable promise in many areas of chemical industry and several domains of engineering.^{1,2} Because of their wide array of applications,^{3–6} they have been receiving considerable attention from a large body of the scientific community.^{7–15}

Shear viscosity (η) is one of the most important and relevant collective properties of ionic liquids. It is a chief characteristic as it is directly related to molecular mobility,¹⁶ which is governed by the size and shape of ions and intermolecular interactions. Lower viscosities are preferred for a solvent so as to increase mass transfer. On the other hand, higher viscosity could be desired for an application such as lubrication. Ionic liquids exhibit a wide range of viscosities at ambient conditions that span many orders of magnitude, in comparison to organic solvents whose viscosity values range from 0.2 to 10 cP.¹⁷ The use of ionic liquids as chemical reaction media or also as electrolytes crucially depends on their viscosity.

The electrochemical stability of an ionic liquid as demonstrated by its large electrochemical potential window is a critical consideration for its use in electrochemistry. In addition, another important property is its electrical conductivity (σ). Electrical conductivity provides a measure of the number of charge carriers and their mobility in the liquid state. An accurate prediction of the electrical conductivity of ILs can be useful in many applications, such as batteries, fuel cells, double-layer capacitors, and dye-sensitized solar cells.^{18,19}

Atomistic simulations have proven useful for accessing less established trends and useful properties of ionic liquids. Because of the slow dynamics of ions and high viscosity of ionic liquids, the accurate prediction of transport properties of ionic liquids from molecular dynamics simulations is computationally very challenging.

Until now, a significant body of simulation studies have been conducted for the computation of viscosities of ionic liquids. The viscosity of ionic liquids has been computed in many different ways, such as equilibrium molecular dynamics simulations,^{20–24} nonequilibrium molecular dynamics,²⁵ and reverse nonequilibrium molecular dynamics simulations.^{26,27} Most of these studies have used force fields that describe static properties reliably well compared to experiment, but not guaranteed to be equally accurate for the prediction of dynamical properties. For example, Yan and co-workers²⁸ used a fixed charge model as well as a polarizable model to determine the viscosity of 1-ethyl-3-methylimidazolium nitrate ($[\text{EMIM}][\text{NO}_3]$) at 400 K from an equilibrium molecular dynamics (MD) simulation. They found the viscosity from simulations to be about 50 % higher than the experimental value in the case of the fixed charge model. However, with the inclusion of electronic polarization, the calculated viscosity showed much better agreement with experiment (within 7 %). Hence, it was concluded that to capture the charge screening effect in ionic liquids which has a large effect on viscosity, one should account for the electronic polarization. The computed viscosity of 1-ethyl-3-methylimidazolium chloride ($[\text{EMIM}][\text{Cl}]$) from the simulation of Rey-Castro and Vega²¹ was around an order of magnitude higher than experimental values over a certain range of temperature. Nonequilibrium MD simulations carried out by Micaelo and co-workers²⁵ on 1-butyl-3-methylimidazolium

Special Issue: Modeling and Simulation of Real Systems

Received: February 8, 2014

Accepted: April 30, 2014

Published: May 8, 2014

hexafluorophosphate ([BMIM][PF₆]) and 1-butyl-3-methylimidazolium nitrate ([BMIM][NO₃]) over a range of temperature provided viscosity values in good agreement with experiment. They employed a fixed charge model and the predicted viscosity was about 10 % lower than the experimental value.

Borodin and Smith²⁹ have used equilibrium MD simulation and a polarizable model to calculate the viscosity of *N*-methyl-*N*-propylpyrrolidinium bis(trifluoromethanesulfonyl)imide ([mpy][NTf₂]) between 303 K and 393 K. The viscosity calculated using the Einstein relation³⁰ underpredicted experimental values by around 25 %. Smit and co-workers developed a united atom model for 1-alkyl-3-methylimidazolium-based ILs with chloride as anion and computed viscosity through equilibrium MD simulations.³¹ The model employed a fractional charge on the ions determined using gas phase quantum calculations. Although the calculated viscosity shown was considerably improved over previous attempts, that of 1-ethyl-3-methylimidazolium chloride predicted from simulation was about 50 % higher than the value measured experimentally.

There have also been a number of simulation studies in which the ionic conductivity of ILs have been computed. Lee and co-workers employed the Nernst–Einstein relation based on the self-diffusion coefficient of ions to obtain the electrical conductivity of few ionic liquids.³² The computed electrical conductivity underestimated experiment by 35 % and 65 % for [BMIM][CF₃SO₃] and [BMIM][PF₆], respectively. Bhargava and Balasubramanian²⁰ computed the electrical conductivity of [MMIM][Cl] at 425 K using both Nernst–Einstein (σ_{NE}) and Green–Kubo (σ_{GK}) relations. The calculated values were 0.012 S cm⁻¹ and 0.0089 S cm⁻¹, respectively, which were much lower compared to the experimental value of 0.106 S cm⁻¹. To study the efficiency of different force fields in the calculation of ionic conductivity, Kolafa and co-workers³³ carried out a series of MD simulations on [PF₆]⁻ and [BF₄]⁻ based ionic liquids using various force fields reported in the literature.^{34–38} They showed that the ratio of conductivity calculated from Green–Kubo and Nernst–Einstein relations lies in the range $0.5 < \sigma_{GK}/\sigma_{NE} < 0.8$. They concluded that the ion motion was partially correlated without prominent ion clustering. Kowsari and co-workers³⁹ carried out MD simulations of 12 1-alkyl-3-methylimidazolium-based ionic liquids using an all atom model³⁴ to examine the transport properties. The computed electrical conductivity values were found to be lower than experimental ones, for example, that for [BMIM][PF₆] was underestimated by 60 % compared to experiment,⁴⁰ whereas for [EMIM][PF₆] and [EMIM][Cl], the simulation results were 68 % and 76 % lower than the experimental data.⁴¹

Very recently, Maginn and co-workers reported the determination of various thermophysical properties of nine ILs obtained by both experiments and computations.⁴² The temperature dependence of thermal conductivity, density, and viscosity were reported. They employed two different sets of atomic site charges within a classical force field framework, one with unit charges, and a second with all atomic charges scaled by 0.8. Results obtained with scaled charges showed better agreement with experiment. The calculated density and heat capacity were in good agreement with experiment, while the thermal conductivities from simulation were slightly higher than experimental values.

In summary, transport properties such as viscosity and electrical conductivity of pure ionic liquids have been computed using atomistic simulations. However, quantitative agreement

with experiments has not been accomplished in many instances. It has been shown that the inclusion of electronic polarizability improves the prediction of transport properties over ones estimated by a fixed charge model. On the other hand, fixed charge force fields are proven to reproduce thermodynamic properties reliably well and are computationally less demanding than polarizable force fields. We have recently proposed a refined, all-atom force field for imidazolium based ionic liquids, where polarization and charge transfer effects in the condensed phases have been captured through the determination of atomic site charges from the crystalline phases of ILs. The DDEC/c3^{43,44} charge partitioning method was employed to deduce the atomic site charges on electronic densities determined using periodic density functional theory (DFT). The calculated total ion charges ranged between 0.6e to 0.8e, depending on the anion. The partial charges thus obtained were utilized within the CLaP³⁴ model. Other force field parameters, such as nonbonded and torsional interactions were refined to reproduce gas phase ion pair interaction energy surfaces. Details of this refinement procedure are described elsewhere.⁴⁵ Seven different ionic liquids were studied using this refined model. Various properties computed using this force field, such as density, heat of vaporization, surface tension and ion diffusion coefficients showed remarkable agreement with experiment.

In this paper, we report the shear viscosity and electrical conductivity for five different ionic liquids. These two transport properties are determined by the decay of time correlation functions of collective quantities and are thus challenging to obtain within simulations. The computed values are compared against experiment wherever such data are available. The decay of stress and electric-current autocorrelation functions are also examined.

The paper is organized as follows. This introduction is followed by details of the methodology employed to calculate transport properties for 1-alkyl-3-methylimidazolium based ionic liquids. The third section is devoted to description of the results obtained which is followed by conclusions.

■ COMPUTATIONAL METHODS

A refined force field for imidazolium based ionic liquids developed recently by us⁴⁵ was employed to model five different ionic liquids: [BMIM][PF₆], [BMIM][BF₄], [BMIM][CF₃SO₃], [BMIM][NTf₂], and [BMIM][NO₃]. Details of interaction potentials of the force field are given elsewhere.⁴⁵ Classical molecular dynamics simulations of these ionic liquids were performed both in the isothermal–isobaric (NPT) and canonical ensemble (NVT) using the LAMMPS⁴⁶ software package. Long-range electrostatic interactions were computed using the particle–particle–mesh (PPPM) solver with a precision of 10⁻⁵. A cutoff of 12 Å was employed to calculate the pairwise interactions in real space. Equations of motion were integrated through the velocity Verlet algorithm with a time step of 1 fs. All C–H covalent bonds were constrained using the SHAKE algorithm as implemented in LAMMPS.⁴⁶ Cross interactions between different atom types were derived using the standard Lorentz–Berthelot rules. Long-range corrections to the calculation of energy and pressure were applied. The temperature and pressure of the systems were maintained at 300 K and 1 atm using a N ose–Hoover thermostat⁴⁷ and barostat, respectively, with a damping factor of 1 ps. Cubic periodic boundary conditions were applied.

The packmol⁴⁸ software package was used to set up the initial configurations. All the systems were simulated using 512 ion pairs. They were equilibrated for 10 ns in the NPT ensemble followed by an analysis trajectory in the constant NVT ensemble. Shear viscosity was calculated through the equilibrium Green–Kubo relation using the full stress (pressure) tensor,⁴⁹

$$\eta(t) = \frac{V}{10k_B T} \int_0^t \langle \text{Tr}[\tilde{\mathbf{P}}(t'')\tilde{\mathbf{P}}(t' + t'')] \rangle dt' \quad (1)$$

where V is the volume of the simulation cell and $\tilde{\mathbf{P}}$ is the symmetric, traceless part of the pressure tensor. Angular brackets denote averaging over t'' . Equation 1 uses all the elements of the pressure tensor and has been found to be more accurate providing a better statistics over the one which uses only the off-diagonal elements⁵⁰ or other nonequilibrium methods.⁵¹

The long time value of the integral in eq 1 yields the shear viscosity, η . The integrand is the stress–stress time correlation function, $C_p(t)$. This autocorrelation function decays rapidly at short times but can exhibit a rather slow decay, thus making the convergence of its integral a tedious one. It is a well-known fact that ionic liquids exhibit sluggish dynamic behavior,⁵² and therefore it is very important to integrate the long time behavior accurately to obtain a reliable value of viscosity. Pressure tensor at every time step was stored from nine independent MD runs each of length 8 ns. The stress–stress autocorrelation function was calculated from the block average of these runs from which the shear viscosity was obtained.

The zero-frequency electrical conductivity, σ was computed using the time integral of electric-current autocorrelation function defined as^{53,54}

$$\sigma = \frac{1}{3k_B T V} \int_0^\infty \langle \mathbf{j}(t) \cdot \mathbf{j}(0) \rangle dt = \frac{1}{3k_B T V} \int_0^\infty J(t) dt \quad (2)$$

where $\mathbf{j}(t)$ is the electric-current function,

$$\mathbf{j}(t) = \sum_{i=1}^N q_i \mathbf{v}_i(t) \quad (3)$$

and q_i and $\mathbf{v}_i(t)$ represent the charge and velocity of atom i at time t . N is the total number of atoms in the system. The electric-current autocorrelation function, $J(t)$ can be expressed as⁵⁵

$$\begin{aligned} J(t) &= \left\langle \sum_{i=1}^N \sum_{j=1}^N q_i q_j \mathbf{v}_i(t) \cdot \mathbf{v}_j(0) \right\rangle \\ &= \left\langle \sum_{i=1}^{N_c} \sum_{j=1}^{N_c} q_i q_j \mathbf{v}_i(t) \cdot \mathbf{v}_j(0) \right\rangle + \left\langle \sum_{i=1}^{N_a} \sum_{j=1}^{N_a} q_i q_j \mathbf{v}_i(t) \cdot \mathbf{v}_j(0) \right\rangle \\ &\quad + \left\langle 2 \sum_{i=1}^{N_c} \sum_{j=1}^{N_a} q_i q_j \mathbf{v}_i(t) \cdot \mathbf{v}_j(0) \right\rangle \\ &= J_{++}(t) + J_{--}(t) + 2J_{+-}(t) \end{aligned} \quad (4)$$

where, N_c and N_a are the number of atoms belonging to all cations and anions, respectively, and $N = N_c + N_a$. The electric current autocorrelation function can thus be expressed as the sum of three terms: J_{++} is the cation electric current autocorrelation function, J_{--} is the anion electric current

autocorrelation function and J_{+-} is the cation–anion electric current cross correlation function.

Atom velocities were stored at every time step from nine independent MD runs each of length of 2 ns. Better statistics in the running integral for electrical conductivity might require averaging over nearly 25 independent trajectories which is beyond the scope of the current manuscript. The electric-current autocorrelation function was calculated from each run and these were averaged. The integral of stress time correlation function required longer duration to converge than what is required for the integral of the electric current time correlation function.

Ionic conductivity can also be calculated using the Nernst–Einstein relation,⁵⁴

$$\sigma_{\text{NE}} = \frac{N_p q^2}{V k_B T} (D^+ + D^-) \quad (5)$$

where V is the volume, temperature is T , the number of ion pairs is N_p , q is the effective net charge of the ions, and k_B is the Boltzmann constant.

The cross correlation function in eq 4 is thus the deviation from ideal Nernst–Einstein behavior (independent ion motion) and provides a measure of ion pairing in the liquids.

RESULTS AND DISCUSSION

Viscosity. The initial decay of the normalized stress–stress time correlation function $C_p(t)$ for [BMIM][PF₆] and [BMIM][BF₄] are shown in Figure 1. The decay of this TCF

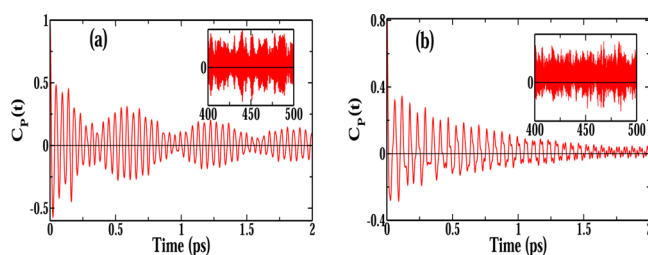


Figure 1. Normalized full stress tensor autocorrelation functions for (a) [BMIM][PF₆] and (b) [BMIM][BF₄] at 300 K. The inset shows the same quantities between 400 and 500 ps.

is characterized by rapid, high amplitude oscillations followed by a slow decay. The oscillations can be inferred as due to the high-frequency intramolecular vibrational modes of the cations. The time scales involved in the relaxation of stress of these systems are evident from the slow decaying nature of $C_p(t)$.

The running integral of the stress correlation function whose converged value corresponds to shear viscosity is plotted for different ionic liquids at 300 K in Figure 2. The values of shear viscosities for all these systems are tabulated in Table 1 and are compared against experimental results. The observed trend in the simulated viscosities is $\eta[\text{BMIM}][\text{PF}_6] > \eta[\text{BMIM}][\text{NO}_3] > \eta[\text{BMIM}][\text{BF}_4] > \eta[\text{BMIM}][\text{CF}_3\text{SO}_3] > \eta[\text{BMIM}][\text{NTf}_2]$. Results from simulation are in good agreement with experiment and follow the same trend.⁵⁶ Gardas and Coutinho⁵⁷ proposed that ionic liquids with highly symmetric, nearly spherical anions are more viscous. In the family of imidazolium based ionic liquids, viscosity increases with anion in the order $[\text{NTf}_2]^- < [\text{CF}_3\text{SO}_3]^- < [\text{BF}_4]^- < [\text{PF}_6]^-$ which trend is reproduced by our simulations. This ranking for different anions can be attributed to both the strength of hydrogen bonding

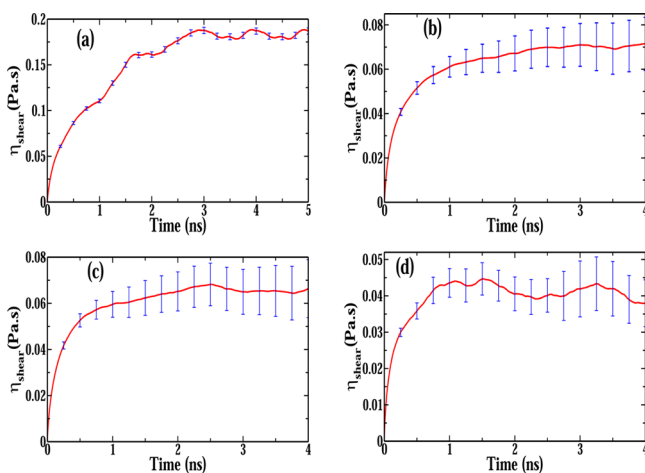


Figure 2. Running integral (see eq 1) representing the shear viscosities of (a) [BMIM][PF₆], (b) [BMIM][BF₄], (c) [BMIM][CF₃SO₃], and (d) [BMIM][NTf₂] from nine independent trajectories at 300 K. The bars are standard error on the mean.

interactions between cation and anion as well as to their electrostatic interaction. Anions in which the negative charge is more delocalized in space exhibit weaker interactions with the cation⁵⁸ and consequently could reduce the viscosity of the IL. Ludwig and co-workers⁵⁹ as well as Hunt⁶⁰ have discussed that hydrogen bonding between cation and anion increases the fluidity of the liquid.

Electrical Conductivity. Electrical conductivity was computed from both the Green–Kubo relation, eq 2 and the Nernst–Einstein relation, eq 5. Self-diffusion coefficients obtained from the slope of mean square displacement (MSD) of individual ions were used to calculate the electrical conductivity from the Nernst–Einstein equation. The self-diffusion coefficient of ions themselves have been reported by us earlier.⁴⁵ Electrical conductivity at 300 K calculated through both these methods are provided in Table 2.

The influence of size, shape, and mass of the anions on the computed electrical conductivities can be observed (see Table 2). Two opposing effects of anions operate in the determination of electrical conductivity. Anions which are larger in size have smaller charge density and consequently exhibit higher mobility. On the other hand, transport of larger anions is not facile because of their large size, which in turn decreases the electrical conductivity.⁴¹ The observed trend in the calculated electrical conductivity is $\sigma[\text{BMIM}][\text{BF}_4] > \sigma[\text{BMIM}][\text{NO}_3] > \sigma[\text{BMIM}][\text{NTf}_2] > \sigma[\text{BMIM}][\text{CF}_3\text{SO}_3] > \sigma[\text{BMIM}][\text{PF}_6]$. From these simulated values, one can see that the conductivity of [BMIM][BF₄] does not follow the

experimentally obtained conductivity order,⁶¹ but for other three ionic liquids it follows the same; for example, this trend is partially supported by the experimental observations of Rivera and co-workers: $\sigma[\text{BMIM}][\text{NTf}_2] > \sigma[\text{BMIM}][\text{CF}_3\text{SO}_3] > \sigma[\text{BMIM}][\text{PF}_6]$.⁶² Among the ILs studied in this work, the one with the [BF₄][−] anion shows the highest electrical conductivity. Table 2 lists conductivities reported in the literature determined through experiments. Reported conductivity values do show variations among themselves (as the temperature at which the experimental measurements were carried out are also different); however, to compare with our simulation results, we have chosen the results obtained by Tokuda et al.,⁶³ as their work also reports some other physical properties (e.g., density, viscosity, etc.) of these ionic liquids which are consistent with previously reported values.

Integration of the electric-current autocorrelation function provides the electrical conductivity through the Green–Kubo relation, eq 2. The electric-current autocorrelation functions were computed from nine independent runs, each of 2 ns in length. In Figure 3, we provide the electric-current autocorrelation functions and their corresponding running integral for [BMIM][PF₆] and [BMIM][NO₃]. The running integral of electric-current autocorrelation functions for other ionic liquids are provided in Figure S5 to Figure S7 in the Supporting Information.

The calculated electrical conductivity values from the Green–Kubo relation shows the same trend as observed from Nernst–Einstein conductivities. Values obtained from the Green–Kubo relation are lower than the Nernst–Einstein conductivity, as the latter method assumes uncorrelated motion of the ions (say, formation of neutral ion clusters) in the liquids. The ratio of σ_{GK} to σ_{NE} gives a measure of correlated ion motion in ionic liquids. In our study, it follows the trend: [BMIM][PF₆] > [BMIM][BF₄] > [BMIM][NO₃] > [BMIM][NTf₂] > [BMIM][CF₃SO₃]. For [BMIM][PF₆], the ion-pair association between cation and anion is the least, whereas for [BMIM][CF₃SO₃], it is the most.

In Figure 4, we show different contributions to the total electric-current correlation function, such as cation–cation, anion–anion, and the cross (cation–anion) correlation functions of [BMIM][PF₆]. The same comparison for other ionic liquids are provided in Figure S1 to Figure S4 in the Supporting Information. In general, the cation–cation current time correlation function decays faster than the corresponding anion–anion one. The magnitude of $J_{+-}(t)$ also is much less than that of $J_{++}(t)$ or $J_{--}(t)$. In an earlier work on [BMIM][Cl], Urahata and Ribeiro⁶⁴ observed that the main contribution to electrical conductivity comes from the anions, while the cross correlation also contributed significantly. The larger diffusion

Table 1. Shear Viscosity (mPa·s) of Ionic Liquids Obtained from Simulation (η_{sim}) Compared against Experimental Data (η_{exp}) at 303 K^a

system	η_{exp}	η_{sim}	$\Delta\eta/\%$	literature data	
				exp	sim
[BMIM][PF ₆]	182.4 ⁶³	185	1.2	209.1, ⁶⁵ 209.2 ⁶⁶	181.8 ²⁵
[BMIM][NO ₃]	123.5 ⁶⁷	129	4.2	144.1 ⁶⁸	135.4 ²⁵
[BMIM][BF ₄]	75.3 ⁶³	71	−5.4	75.4, ⁶⁵ 73.42, ⁶⁹	98 ⁷⁰
[BMIM][CF ₃ SO ₃]	65.4 ⁶³	65	−0.3	63.19, ⁷¹ 64.2 ⁶⁸	90 ⁷²
[BMIM][NTf ₂]	40.0 ⁶³	42	3.7	40.6, ⁶⁵ 40.64 ⁷³	65.1 ⁷⁴

^aEstimated standard error on the mean in η_{sim} is around 5 mPa·s. Values determined from other experimental (303 K) and simulation (298 K) reports are also provided.

Table 2. Electrical Conductivity ($\text{S}\cdot\text{m}^{-1}$) of Ionic Liquids at 300 K Obtained from Simulation (σ_{GK}) Compared against Experimental (σ_{exp}) Data at 303 K^a

system	σ_{exp}	σ_{GK}	σ_{NE}	$\sigma_{\text{GK}}/\sigma_{\text{NE}}$	$\Delta\sigma/\%$	literature data	
						exp	sim
[BMIM][BF ₄]	0.45 ⁶³	0.42	0.51	0.82	-6.6	0.35, ⁷⁵ 0.36 ⁷⁶	0.28 ⁷²
[BMIM][NTf ₂]	0.46 ⁶³	0.29	0.38	0.76	-36.9	0.45, ⁷⁷ 0.39 ⁷⁸	0.42 ⁷²
[BMIM][CF ₃ SO ₃]	0.36 ⁶³	0.25	0.36	0.69	-30.5	0.23, ^{79,b} 0.29 ⁸⁰	0.20 ⁷²
[BMIM][PF ₆]	0.19 ⁶³	0.17	0.19	0.89	-10.5	0.15, ⁷⁷ 0.15 ⁷⁵	0.08 ⁷²
[BMIM][NO ₃]		0.31	0.39	0.79			0.07 ⁷²

^aEstimated standard error on the mean in the simulated value is around $0.05 \text{ S}\cdot\text{m}^{-1}$. Literature data are at 298 K. ^b303 K.

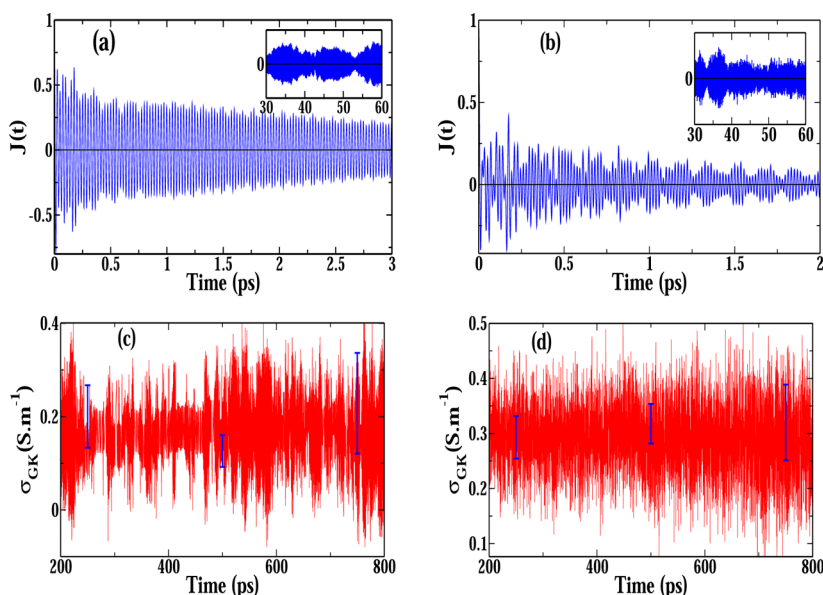


Figure 3. Normalized electric-current autocorrelation functions of (a) [BMIM][PF₆] and (b) [BMIM][NO₃]. Inset shows the magnified region of these autocorrelation functions between 30 ps and 60 ps. Running integral representing electrical conductivity of (c) [BMIM][PF₆] and (d) [BMIM][NO₃]. The bars are standard error on the mean.

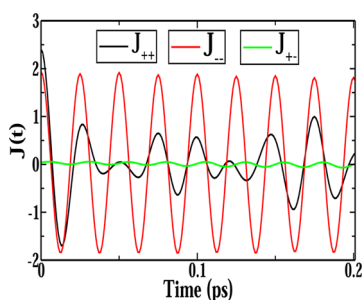


Figure 4. Electric-current correlation functions for cation–cation, anion–anion, and cation–anion of liquid [BMIM][PF₆] at 300 K.

coefficients of chloride ion than that of the cation could be a reason for this observation. In the current study, we observe the contribution from cations and anions to be almost the same.

The center of mass electric-current correlation functions defined as

$$J^{\text{COM}}(t) = \left\langle \sum_{i=1}^{N_p} \sum_{j=1}^{N_p} q_i q_j \mathbf{v}_i^{\text{COM}}(t) \cdot \mathbf{v}_j^{\text{COM}}(0) \right\rangle \quad (6)$$

where, $\mathbf{v}_i^{\text{COM}}$ is the velocity of the center of mass of ion i and N_p is the number of ion pairs.

The center of mass cation–cation (J_{++}^{COM}) and cation–anion electric-current correlation function (J_{+-}^{COM}) for different ionic liquids are compared in Figure 5 at 300 K. The former function

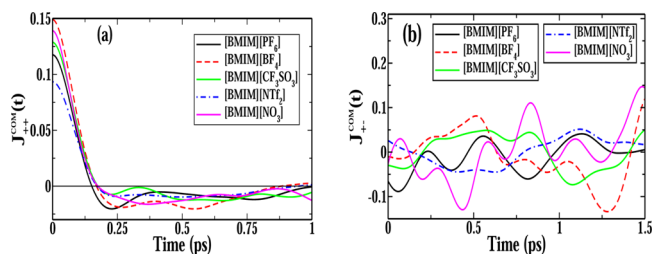


Figure 5. Center of mass (a) cation–cation and (b) cation–anion (cross) electric-current autocorrelation functions of different ionic liquids at 300 K.

exhibits oscillations with different frequencies which arises from different vibrational modes in the cation. J_{++}^{COM} for [BMIM][PF₆] shows the deepest first minimum indicating the strength of the anion cage within which the cation rattles. In a similar fashion, the electric current time correlation function, $J(t)$ can also be recognized as the sum of $J_{++}(t)$, $J_{--}(t)$ and $2J_{+-}(t)$. The integral of these quantities were found to be nearly identical (see Table S1 in Supporting Information), signifying that all of them contribute equally to the electrical conductivity. To

understand this further, we computed the normalized cation–cation velocity autocorrelation functions for different liquids (Figure 6). $[\text{PF}_6]^-$ anion forms the strongest cage among all

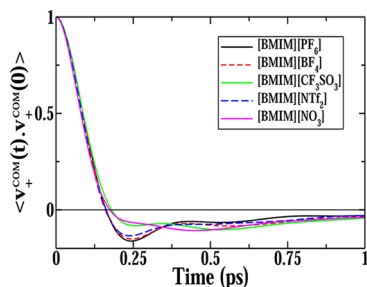


Figure 6. Center of mass velocity autocorrelation functions of cations for different ionic liquids at 300 K.

anions, inside which the cation resides. This is likely the reason for the high viscosity of $[\text{BMIM}][\text{PF}_6]$ compared to other ionic liquids. The sign and magnitude of the first peak of the cross-correlation term (Figure 5b) provides an idea of cation–anion pairing at short times.³⁹ The most negative value is seen for $[\text{BMIM}][\text{PF}_6]$ which implies that the anions forming the cage around a cation move in a concerted manner (i.e., they have the same direction of center of mass velocity)

Temperature Dependence of Electrical Conductivity.

In this subsection, we discuss the temperature dependence of the electrical conductivity for four liquids. To this end, electrical conductivities were derived using the Green–Kubo relation (eq 2) at temperatures $T = (300, 330, 360, \text{ and } 400)$ K for $[\text{BMIM}][\text{PF}_6]$ and $[\text{BMIM}][\text{BF}_4]$, while for $[\text{BMIM}][\text{CF}_3\text{SO}_3]$ and $[\text{BMIM}][\text{NTf}_2]$, the conductivities were calculated at $T = (330, 333, 353, \text{ and } 373)$ K.

In Figure 7, electrical conductivity obtained from simulations are compared against experimental results at different temper-

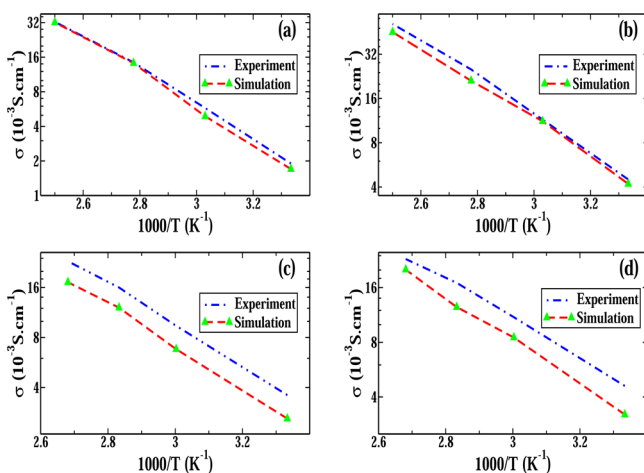


Figure 7. Electrical conductivity obtained from simulations compared against experimental data⁶³ (a) $[\text{BMIM}][\text{PF}_6]$, (b) $[\text{BMIM}][\text{BF}_4]$, (c) $[\text{BMIM}][\text{CF}_3\text{SO}_3]$, and (d) $[\text{BMIM}][\text{NTf}_2]$.

atures. For $[\text{BMIM}][\text{PF}_6]$ and $[\text{BMIM}][\text{BF}_4]$, the simulations reproduce experimental data rather well over the entire temperature range. The calculated results for $[\text{BMIM}][\text{CF}_3\text{SO}_3]$ and $[\text{BMIM}][\text{NTf}_2]$ are within 30 % of experiment, and the temperature dependence is well reproduced.

CONCLUSIONS

Classical molecular dynamics simulations have been carried out for five room temperature ionic liquids, all based on the 1-butyl-3-methylimidazolium cation using a force field developed recently.⁴⁵ The potential model represented ions with partial charges which were determined from quantum calculations of crystal structures of compounds of room temperature ionic liquids. The force field, although a nonpolarizable one, was demonstrated to predict the self-diffusion coefficient of ions in quantitative agreement with experiment.⁴⁵

Here, we have calculated collective transport properties, such as shear viscosity and electrical conductivity of five ILs at 300 K. The equilibrium Green–Kubo relation was employed to calculate the shear viscosity from the long-time integral of stress–stress autocorrelation functions of different ionic liquids. A similar procedure adopted with the electric-current autocorrelation function yielded the electrical conductivities. An estimate of correlated ion motion in these liquids was obtained through a comparison of the Green–Kubo and Nernst–Einstein conductivities. The force field is able to reproduce the experimental values of shear viscosity of these liquids rather accurately. The prediction of electrical conductivity of $[\text{BMIM}][\text{PF}_6]$ and $[\text{BMIM}][\text{BF}_4]$ is remarkably good while that for $[\text{BMIM}][\text{CF}_3\text{SO}_3]$ and $[\text{BMIM}][\text{NTf}_2]$ is fair. Reconciliation of the conductivity of the latter between simulation and experiments needs further study.

Cation–anion electric current cross correlation functions decay faster than cation–cation or anion–anion correlation functions. The cation–anion electric current cross correlation function for $[\text{BMIM}][\text{PF}_6]$ exhibited the most negative value at zero time signifying the concerted motion of an ion with its counterion cage at short-times.

The accuracy with which this nonpolarizable force field reproduces collective transport quantities such as shear viscosity or electrical conductivity provides us confidence to apply the force field development protocol to other novel ionic liquids. This approach will constitute our endeavor in the near future.

ASSOCIATED CONTENT

Supporting Information

Additional figures and table as described in the text. This material is available free of charge via the Internet at <http://pubs.acs.org>.

AUTHOR INFORMATION

Corresponding Author

*E-mail: bala@jncasr.ac.in.

Funding

We thank DST, India for support. S.B. thanks Sheikh Saqr Laboratory, JNCASR for a senior fellowship.

Notes

The authors declare no competing financial interest.

REFERENCES

- (1) Sheldon, R. A. Green solvents for sustainable organic synthesis: State of the art. *Green Chem.* **2005**, *7*, 267–278.
- (2) Plechkova, N. V.; Seddon, K. R. Applications of ionic liquids in the chemical industry. *Chem. Soc. Rev.* **2008**, *37*, 123–150.
- (3) Jovanovski, V.; González-Pedro, V.; Giménez, S.; Azaceta, E.; Cabañero, G.; Grande, H.; Tena-Zaera, R.; Mora-Seró, I.; Bisquert, J. A Sulfide/Polysulfide-Based Ionic Liquid Electrolyte for Quantum Dot-Sensitized Solar Cells. *J. Am. Chem. Soc.* **2011**, *133*, 20156–20159.

- (4) Kim, H.; Ding, Y.; Kohl, P. A. LiSICON—Ionic liquid electrolyte for lithium ion battery. *J. Power Sources* **2012**, *198*, 281–286.
- (5) Lin, R.; Taberna, P.-L.; Fantini, S.; Presser, V.; Pérez, C. R.; Malbosc, F.; Rupasinghe, N. L.; Teo, K. B. K.; Gogotsi, Y.; Simon, P. Capacitive Energy Storage from –50 to 100 °C Using an Ionic Liquid Electrolyte. *J. Phys. Chem. Lett.* **2011**, *2*, 2396–2401.
- (6) Zhang, D.; Chang, W. C.; Okajima, T.; Ohsaka, T. Electrodeposition of Platinum Nanoparticles in a Room-Temperature Ionic Liquid. *Langmuir* **2011**, *27*, 14662–14668.
- (7) Dupont, J. From Molten Salts to Ionic Liquids: A “Nano” Journey. *Acc. Chem. Res.* **2011**, *44*, 1223–1231.
- (8) Maginn, E. J. Atomistic Simulation of the Thermodynamic and Transport Properties of Ionic Liquids. *Acc. Chem. Res.* **2007**, *40*, 1200–1207.
- (9) Maginn, E. J. Molecular simulation of ionic liquids: Current status and future opportunities. *J. Phys.: Condens. Matter* **2009**, *21*, 373101.
- (10) Brennecke, J. F.; Gurkan, B. E. Ionic Liquids for CO₂ Capture and Emission Reduction. *J. Phys. Chem. Lett.* **2010**, *1*, 3459–3464.
- (11) Niedermeyer, H.; Hallett, J. P.; Villar-Garcia, I. J.; Hunt, P. A.; Welton, T. Mixtures of Ionic Liquids. *Chem. Soc. Rev.* **2012**, *41*, 7780–7802.
- (12) Gurkan, B.; Goodrich, B. F.; Mindrup, E. M.; Ficke, L. E.; Massel, M.; Seo, S.; Senftle, T. P.; Wu, H.; Glaser, M. F.; Shah, J. K.; Maginn, E. J.; Brennecke, J. F.; Schneider, W. F. Molecular Design of High Capacity, Low Viscosity, Chemically Tunable Ionic Liquids for CO₂ Capture. *J. Phys. Chem. Lett.* **2010**, *1*, 3494–3499.
- (13) Harris, K. R.; Kanakubo, M.; Woolf, L. A. Temperature and Pressure Dependence of the Viscosity of the Ionic Liquids 1-Hexyl-3-methylimidazolium Hexafluorophosphate and 1-Butyl-3-methylimidazolium Bis(trifluoromethylsulfanyl)imide. *J. Chem. Eng. Data* **2007**, *52*, 1080–1085.
- (14) Kanakubo, M.; Harris, K. R.; Tsuchihashi, N.; Ibuki, K.; Ueno, M. Effect of Pressure on Transport Properties of the Ionic Liquid 1-Butyl-3-methylimidazolium Hexafluorophosphate. *J. Phys. Chem. B* **2007**, *111*, 2062–2069.
- (15) Harris, K. R.; Kanakubo, M.; Woolf, L. A. Temperature and Pressure Dependence of the Viscosity of the Ionic Liquid 1-Butyl-3-methylimidazolium Tetrafluoroborate: Viscosity and Density Relationships in Ionic Liquids. *J. Chem. Eng. Data* **2007**, *52*, 2425–2430.
- (16) Yamaguchi, T.; Miyake, S.; Koda, S. Shear Relaxation of Imidazolium-Based Room-Temperature Ionic Liquids. *J. Phys. Chem. B* **2010**, *114*, 8126–8133.
- (17) Shirota, H.; Castner, E. W. Why Are Viscosities Lower for Ionic Liquids with –CH₂Si(CH₃)₃ vs –CH₂C(CH₃)₃ Substitutions on the Imidazolium Cations? *J. Phys. Chem. B* **2005**, *109*, 21576–21585.
- (18) Crosthwaite, J. M.; Muldoon, M. J.; Dixon, J. K.; Anderson, J. L.; Brennecke, J. F. Phase Transition and Decomposition Temperatures, Heat Capacities and Viscosities of Pyridinium Ionic Liquids. *J. Chem. Thermodyn.* **2005**, *37*, 559–568.
- (19) Buzzeo, M. C.; Evans, R. G.; Compton, R. G. Non-Haloaluminate Room-Temperature Ionic Liquids in Electrochemistry—A Review. *ChemPhysChem* **2004**, *5*, 1106–1120.
- (20) Bhargava, B. L.; Balasubramanian, S. Dynamics in a Room-Temperature Ionic Liquid: A Computer Simulation Study of 1,3-Dimethylimidazolium Chloride. *J. Chem. Phys.* **2005**, *123*, 144505.
- (21) Rey-Castro, C.; Vega, L. F. Transport Properties of the Ionic Liquid 1-Ethyl-3-Methylimidazolium Chloride from Equilibrium Molecular Dynamics Simulation. The Effect of Temperature. *J. Phys. Chem. B* **2006**, *110*, 14426–14435.
- (22) Rey-Castro, C.; Tormo, A.; Vega, L. Effect of the Flexibility and the Anion in the Structural and Transport Properties of Ethyl-Methyl-Imidazolium Ionic Liquids. *Fluid Phase Equilib.* **2007**, *256*, 62–69.
- (23) Borodin, O.; Smith, G. D.; Kim, H. Viscosity of a Room Temperature Ionic Liquid: Predictions from Nonequilibrium and Equilibrium Molecular Dynamics Simulations. *J. Phys. Chem. B* **2009**, *113*, 4771–4774.
- (24) Butler, S. N.; Müller-Plathe, F. A Molecular Dynamics Study of Viscosity in Ionic Liquids Directed by Quantitative Structure-Property Relationships. *ChemPhysChem* **2012**, *13*, 1791–1801.
- (25) Micaelo, N. M.; Baptista, A. M.; Soares, C. M. Parametrization of 1-Butyl-3-methylimidazolium Hexafluorophosphate/Nitrate Ionic Liquid for the GROMOS Force Field. *J. Phys. Chem. B* **2006**, *110*, 14444–14451.
- (26) Kelkar, M. S.; Maginn, E. J. Effect of Temperature and Water Content on the Shear Viscosity of the Ionic Liquid 1-Ethyl-3-methylimidazolium Bis(trifluoromethanesulfonyl)imide as Studied by Atomistic Simulations. *J. Phys. Chem. B* **2007**, *111*, 4867–4876.
- (27) Zhao, W.; Leroy, F.; Balasubramanian, S.; Müller-Plathe, F. Shear Viscosity of the Ionic Liquid 1-*n*-Butyl 3-Methylimidazolium Hexafluorophosphate [bmim][PF₆] Computed by Reverse Non-equilibrium Molecular Dynamics. *J. Phys. Chem. B* **2008**, *112*, 8129–8133.
- (28) Yan, T.; Burnham, C. J.; Del Pópolo, M. G.; Voth, G. A. Molecular Dynamics Simulation of Ionic Liquids: The Effect of Electronic Polarizability. *J. Phys. Chem. B* **2004**, *108*, 11877–11881.
- (29) Borodin, O.; Smith, G. D. Structure and Dynamics of *N*-Methyl-*N*-propylpyrrolidinium Bis(trifluoromethanesulfonyl)imide Ionic Liquid from Molecular Dynamics Simulations. *J. Phys. Chem. B* **2006**, *110*, 11481–11490.
- (30) Allen, M. P.; Tildesley, D. J. *Computer Simulation of Liquids*; Oxford Science Publications; Oxford University Press, USA, 1989.
- (31) Liu, Z.; Chen, T.; Bell, A.; Smit, B. Improved United-Atom Force Field for 1-Alkyl-3-methylimidazolium Chloride. *J. Phys. Chem. B* **2010**, *114*, 4572–4582.
- (32) Lee, S. U.; Jung, J.; Han, Y.-K. Molecular Dynamics Study of the Ionic Conductivity of 1-*n*-Butyl-3-methylimidazolium Salts as Ionic Liquids. *Chem. Phys. Lett.* **2005**, *406*, 332–340.
- (33) Picálek, J.; Kolafa, J. Molecular dynamics Study of Conductivity of Ionic Liquids: The Kohlrausch Law. *J. Mol. Liq.* **2007**, *134*, 29–33.
- (34) Canongia Lopes, J. N.; Deschamps, J.; Pádua, A. A. H. Modeling Ionic Liquids Using a Systematic All-Atom Force Field. *J. Phys. Chem. B* **2004**, *108*, 2038–2047.
- (35) Hanke, C. G.; Price, S. L.; Lynden-Bell, R. M. Intermolecular Potentials for Simulations of Liquid Imidazolium Salts. *Mol. Phys.* **2001**, *99*, 801–809.
- (36) Liu, Z.; Huang, S.; Wang, W. A Refined Force Field for Molecular Simulation of Imidazolium-Based Ionic Liquids. *J. Phys. Chem. B* **2004**, *108*, 12978–12989.
- (37) Urahata, S. M.; Ribeiro, M. C. C. Structure of Ionic Liquids of 1-Alkyl-3-methylimidazolium Cations: A Systematic Computer Simulation Study. *J. Chem. Phys.* **2004**, *120*, 1855–1863.
- (38) Shah, J. K.; Brennecke, J. F.; Maginn, E. J. Thermodynamic Properties of the Ionic Liquid 1-*n*-Butyl-3-methylimidazolium Hexafluorophosphate from Monte Carlo Simulations. *Green Chem.* **2002**, *4*, 112–118.
- (39) Kowsari, M. H.; Alavi, S.; Ashrafzaadeh, M.; Najafi, B. Molecular Dynamics Simulation of Imidazolium-Based Ionic Liquids. II. Transport Coefficients. *J. Chem. Phys.* **2009**, *130*, 014703.
- (40) Zech, O.; Stoppa, A.; Buchner, R.; Kunz, W. The Conductivity of Imidazolium-Based Ionic Liquids from (248 to 468) K. B. Variation of the Anion. *J. Chem. Eng. Data* **2010**, *55*, 1774–1778.
- (41) Vila, J.; Varela, L.; Cabeza, O. Cation and Anion Sizes Influence in the Temperature Dependence of the Electrical Conductivity in Nine Imidazolium Based Ionic Liquids. *Electrochim. Acta* **2007**, *52*, 7413–7417.
- (42) Tenney, C. M.; Massel, M.; Mayes, J. M.; Sen, M.; Brennecke, J. F.; Maginn, E. J. A Computational and Experimental Study of the Heat Transfer Properties of Nine Different Ionic Liquids. *J. Chem. Eng. Data* **2014**, *59*, 391–399, DOI: 10.1021/je400858t.
- (43) Manz, T. A.; Sholl, D. S. Improved Atoms-in-Molecule Charge Partitioning Functional for Simultaneously Reproducing the Electrostatic Potential and Chemical States in Periodic and Nonperiodic Materials. *J. Chem. Theory Comput.* **2012**, *8*, 2844–2867.
- (44) Manz, T. A.; Sholl, D. S. Chemically Meaningful Atomic Charges That Reproduce the Electrostatic Potential in Periodic and Nonperiodic Materials. *J. Chem. Theory Comput.* **2010**, *6*, 2455–2468.
- (45) Mondal, A.; Balasubramanian, S. Quantitative Prediction of Physical Properties of Imidazolium Based Room Temperature Ionic

Liquids through Determination of Condensed Phase Site Charges: A Refined Force Field. *J. Phys. Chem. B* **2014**, *118*, 3409–3422.

(46) Plimpton, S. Fast Parallel Algorithms for Short-Range Molecular Dynamics. *J. Comput. Phys.* **1995**, *117*, 1–19.

(47) Hoover, W. G. Canonical Dynamics: Equilibrium Phase-Space Distributions. *Phys. Rev. A* **1985**, *31*, 1695–1697.

(48) Martínez, L.; Andrade, R.; Birgin, E. G.; Martínez, J. M. PACKMOL: A Package for Building Initial Configurations for Molecular Dynamics Simulations. *J. Comput. Chem.* **2009**, *30*, 2157–2164.

(49) Davis, P. J.; Evans, D. J. Comparison of Constant Pressure and Constant Volume Nonequilibrium Simulations of Sheared Model Decane. *J. Chem. Phys.* **1994**, *100*, 541–547.

(50) Mundy, C. J.; Siepmann, J. I.; Klein, M. L. Decane under Shear: A Molecular Dynamics Study Using Reversible NVT-SLLOD and NPT-SLLOD Algorithms. *J. Chem. Phys.* **1995**, *103*, 10192–10200.

(51) Chen, T.; Smit, B.; Bell, A. T. Are Pressure Fluctuation-Based Equilibrium Methods Really Worse than Nonequilibrium Methods for Calculating Viscosities? *J. Chem. Phys.* **2009**, *131*, 246101.

(52) Sarangi, S. S.; Zhao, W.; Müller-Plathe, F.; Balasubramanian, S. Correlation between Dynamic Heterogeneity and Local Structure in a Room-Temperature Ionic Liquid: A Molecular Dynamics Study of [bmim][PF₆]. *ChemPhysChem* **2010**, *11*, 2001–2010.

(53) Harada, M.; Yamanaka, A.; Tanigaki, M.; Tada, Y. Mass and Size Effects on the Transport Properties of Molten Salts. *J. Chem. Phys.* **1982**, *76*, 1550–1556.

(54) Hansen, J.-P.; McDonald, I. R. *Theory of Simple Liquids*, 3rd ed.; Academic Press: San Diego, CA, 2006.

(55) Del Pópolo, M. G.; Voth, G. A. On the Structure and Dynamics of Ionic Liquids. *J. Phys. Chem. B* **2004**, *108*, 1744–1752.

(56) Jin, H.; O'Hare, B.; Dong, J.; Arzhantsev, S.; Baker, G. A.; Wishart, J. F.; Benesi, A. J.; Maroncelli, M. Physical Properties of Ionic Liquids Consisting of the 1-Butyl-3-methylimidazolium Cation with Various Anions and the Bis(trifluoromethylsulfonyl)imide Anion with Various Cations. *J. Phys. Chem. B* **2008**, *112*, 81–92.

(57) Gardas, R. L.; Coutinho, J. A. A Group Contribution Method for Viscosity Estimation of Ionic Liquids. *Fluid Phase Equilib.* **2008**, *266*, 195–201.

(58) Bonhôte, P.; Dias, A.-P.; Papageorgiou, N.; Kalyanasundaram, K.; Grätzel, M. Hydrophobic, Highly Conductive Ambient-Temperature Molten Salts. *Inorg. Chem.* **1996**, *35*, 1168–1178.

(59) Fumino, K.; Peppel, T.; Geppert-Rybczynska, M.; Zaitsau, D. H.; Lehmann, J. K.; Verevkin, S. P.; Kockerling, M.; Ludwig, R. The Influence of Hydrogen Bonding on the Physical Properties of Ionic Liquids. *Phys. Chem. Chem. Phys.* **2011**, *13*, 14064–14075.

(60) Hunt, P. A. Why Does a Reduction in Hydrogen Bonding Lead to an Increase in Viscosity for the 1-Butyl-2,3-dimethyl-imidazolium-Based Ionic Liquids? *J. Phys. Chem. B* **2007**, *111*, 4844–4853.

(61) Tokuda, H.; Hayamizu, K.; Ishii, K.; Susan, M. A. B. H.; Watanabe, M. Physicochemical Properties and Structures of Room Temperature Ionic Liquids. 1. Variation of Anionic Species. *J. Phys. Chem. B* **2004**, *108*, 16593–16600.

(62) Rivera, A.; Brodin, A.; Pugachev, A.; Rössler, E. A. Orientational and Translational Dynamics in Room Temperature Ionic Liquids. *J. Chem. Phys.* **2007**, *126*, 114503.

(63) Tokuda, H.; Tsuzuki, S.; Susan, M. A. B. H.; Hayamizu, K.; Watanabe, M. How Ionic Are Room-Temperature Ionic Liquids? An Indicator of the Physicochemical Properties. *J. Phys. Chem. B* **2006**, *110*, 19593–19600.

(64) Urahata, S. M.; Ribeiro, M. C. C. Collective Excitations in an Ionic Liquid. *J. Chem. Phys.* **2006**, *124*, 074513.

(65) Jacquemin, J.; Husson, P.; Padua, A. A. H.; Majer, V. Density and Viscosity of Several Pure and Water-Saturated Ionic Liquids. *Green Chem.* **2006**, *8*, 172–180.

(66) Fan, W.; Zhou, Q.; Sun, J.; Zhang, S. Density, Excess Molar Volume, and Viscosity for the Methyl Methacrylate + 1-Butyl-3-methylimidazolium Hexafluorophosphate Ionic Liquid Binary System at Atmospheric Pressure. *J. Chem. Eng. Data* **2009**, *54*, 2307–2311.

(67) Mokhtarani, B.; Sharifi, A.; Mortaheb, H. R.; Mirzaei, M.; Mafi, M.; Sadeghian, F. Density and Viscosity of 1-Butyl-3-methylimidazolium Nitrate with Ethanol, 1-Propanol, or 1-Butanol at Several Temperatures. *J. Chem. Thermodyn.* **2009**, *41*, 1432–1438.

(68) Seddon, K. R.; Annegret, S.; María-José, T. *Clean Solvents*; American Chemical Society: Washington, DC, 2002; Chapter 5, pp 34–49.

(69) Vakili-Nezhaad, G.; Vatani, M.; Asghari, M.; Ashour, I. Effect of Temperature on the Physical Properties of 1-Butyl-3-Methylimidazolium Based Ionic Liquids with Thiocyanate and Tetrafluoroborate Anions, and 1-Hexyl-3-Methylimidazolium with Tetrafluoroborate and Hexafluorophosphate Anions. *J. Chem. Thermodyn.* **2012**, *54*, 148–154.

(70) Chaban, V. V.; Voroshylova, I. V.; Kalugin, O. N.; Prezhdo, O. V. Acetonitrile Boosts Conductivity of Imidazolium Ionic Liquids. *J. Phys. Chem. B* **2012**, *116*, 7719–7727.

(71) Ge, M.-L.; Zhao, R.-S.; Yi, Y.-F.; Zhang, Q.; Wang, L.-S. Densities and Viscosities of 1-Butyl-3-methylimidazolium Trifluoromethanesulfonate + H₂O Binary Mixtures at T = (303.15 to 343.15) K. *J. Chem. Eng. Data* **2008**, *53*, 2408–2411.

(72) Borodin, O. Polarizable Force Field Development and Molecular Dynamics Simulations of Ionic Liquids. *J. Phys. Chem. B* **2009**, *113*, 11463–11478.

(73) Katsuta, S.; Shiozawa, Y.; Imai, K.; Kudo, Y.; Takeda, Y. Stability of Ion Pairs of Bis(trifluoromethanesulfonyl)amide-Based Ionic Liquids in Dichloromethane. *J. Chem. Eng. Data* **2010**, *55*, 1588–1593.

(74) Androulaki, E.; Vergadou, N.; Ramos, J.; Economou, I. G. Structure, Thermodynamic and Transport Properties of Imidazolium-Based Bis(trifluoromethylsulfonyl)imide Ionic Liquids from Molecular Dynamics Simulations. *Mol. Phys.* **2012**, *110*, 1139–1152.

(75) Stoppa, A.; Hunger, J.; Buchner, R. Conductivities of Binary Mixtures of Ionic Liquids with Polar Solvents. *J. Chem. Eng. Data* **2009**, *54*, 472–479.

(76) Schreiner, C.; Zugmann, S.; Hartl, R.; Gores, H. J. Fractional Walden Rule for Ionic Liquids: Examples from Recent Measurements and a Critique of the So-Called Ideal KCl Line for the Walden Plot. *J. Chem. Eng. Data* **2010**, *55*, 1784–1788.

(77) Widegren, J. A.; Saurer, E. M.; Marsh, K. N.; Magee, J. W. Electrolytic Conductivity of Four Imidazolium-Based Room-Temperature Ionic Liquids and the Effect of a Water Impurity. *J. Chem. Thermodyn.* **2005**, *37*, 569–575.

(78) Vranes, M.; Dozic, S.; Djeric, V.; Gadzuric, S. Physicochemical Characterization of 1-Butyl-3-methylimidazolium and 1-Butyl-1-methylpyrrolidinium Bis(trifluoromethylsulfonyl)imide. *J. Chem. Eng. Data* **2012**, *57*, 1072–1077.

(79) Yu, Y.-H.; Soriano, A. N.; Li, M.-H. Heat Capacities and Electrical Conductivities of 1-*n*-Butyl-3-methylimidazolium-Based Ionic Liquids. *Thermochim. Acta* **2009**, *482*, 42–48.

(80) Zech, O.; Stoppa, A.; Buchner, R.; Kunz, W. The Conductivity of Imidazolium-Based Ionic Liquids from (248 to 468) K. B. Variation of the Anion. *J. Chem. Eng. Data* **2010**, *55*, 1774–1778.